

FoodLogAthl-218: Constructing a Real-World Food Image Dataset Using Dietary Management Applications

Mitsuki Watanabe
The University of Tokyo
Tokyo, Japan
watanabe@hal.t.u-tokyo.ac.jp

Kiyoharu Aizawa
The University of Tokyo
Tokyo, Japan
aizawa@hal.t.u-tokyo.ac.jp

Sosuke Amano
foo.log Inc.
Tokyo, Japan
amano@foo-log.co.jp

Yoko Yamakata
The University of Tokyo
Tokyo, Japan
yamakata@hal.t.u-tokyo.ac.jp

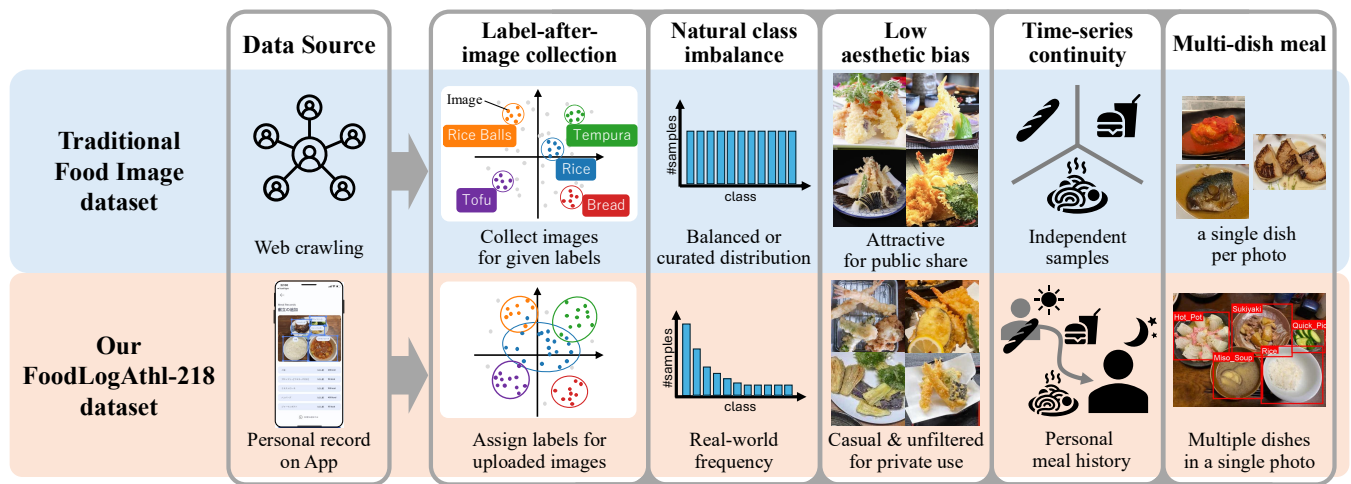


Figure 1: Comparison between traditional food image datasets and FoodLogAthl-218.

Abstract

Food image classification models are crucial for dietary management applications because they reduce the burden of manual meal logging. However, most publicly available datasets for training such models rely on web-crawled images, which often differ from users' real-world meal photos. In this work, we present *FoodLogAthl-218*, a food image dataset constructed from real-world meal records collected through the dietary management application FoodLog Athl. The dataset contains 6,925 images across 218 food categories, with a total of 14,349 bounding boxes. Rich metadata, including meal date and time, anonymized user IDs, and meal-level context, accompany each image. Unlike conventional datasets—where a predefined class set guides web-based image collection—our data begins with user-submitted photos, and labels are applied afterward. This yields greater intra-class diversity, a natural frequency distribution of meal types, and casual, unfiltered images intended for personal use rather than public sharing. In addition to (1) a standard classification benchmark, we introduce two FoodLog-specific tasks: (2) an incremental fine-tuning protocol that follows the temporal stream of users' logs,

and (3) a context-aware classification task where each image contains multiple dishes, and the model must classify each dish by leveraging the overall meal context. We evaluate these tasks using large multimodal models (LMMs). The dataset is publicly available at <https://huggingface.co/datasets/FoodLog/FoodLogAthl-218>.

CCS Concepts

• Computing methodologies → Computer vision tasks; • Applied computing → Health care information systems; • Information systems → Data management systems.

Keywords

food image dataset; food management application; personal food record; time-series meal logs; multi-dish meal images

1 Introduction

Most publicly available food-category classification datasets are built from web-sourced images [5, 9, 10, 19, 21, 26–28, 35, 36, 38–40, 42, 45, 50, 53]. Although some studies utilize proprietary food logs, these datasets are typically not publicly available due to privacy and licensing constraints [4, 20, 29].

To address this gap, we constructed and publicly released a new food image dataset, **FoodLogAthl-218**, based on users' personal

This is the authors' preprint version of the paper accepted to ACM Multimedia 2025 (Dataset Track). The official version is available at: <https://doi.org/10.1145/3746027.3758276>.

Table 1: Comparison of Datasets for Food Image Classification Tasks.

Year	Dataset Name	#classes	#samples	Cuisine Category	Data Source
2009	PFID [12]	101	4,545	Western	Fast Food Chains
2014	UEC-Food 256 [28]	256	25,088	International	Web + Original Database
2014	Food-101 [10]	101	101,000	Western	Web (foodspotting.com)
2015	UPMC Food-101 [50]	101	90,840	Western	Web (Google [17])
2016	UNICT-FD1200 [16]	1,200	4,754	International	Experiment Participants
2017	Vegfru [21]	25/292*	160,000	Vegetables, Fruits	Web (Google, ImageNet [14], etc.)
2019	FoodAI-756 [45]	152/756*	400,000	International	Web (Google, Bing, etc.)
2021	Food2K [40]	2,000	1,036,564	International	Web (Meituan [37])
2023	Food-500 Cap [35]	494	24,700	International	Web (Google, Bing)
2025	FoodLogAthl-218	218	14,349	International	Dietary Management App

* Hierarchically structured dataset, where n/m indicates m classes divided into n higher-level classes.

food records collected via a food management application we developed. The dataset was curated with approval from our institutional ethics board; informed consent was obtained from all participants, and personally identifiable information was removed via a two-stage manual process. Since the raw user-submitted data included missing or incorrect detections and noisy labels, we applied a custom multi-stage filtering pipeline to produce a clean, research-ready subset consisting of 6,925 images and 14,349 bounding boxes across 218 food categories—comparable in scope to existing classification datasets.

The **FoodLogAthl-218** dataset introduces the following five key properties that distinguish it from existing food image benchmarks and make it better suited for real-world dietary logging scenarios. **Label-after-image collection** Unlike most existing datasets, where a fixed set of class labels is defined first, and images are then collected to match those labels, our dataset begins with user-submitted meal photos, which are labeled post hoc. This bottom-up process yields significantly higher intra-class diversity and more accurately reflects the nature of real-world food logging tasks.

Natural class imbalance While existing datasets often attempt to balance the number of samples per class or rely on the availability of web-sourced images, our dataset preserves the natural frequency distribution of meals as they appear in everyday food records.

Low aesthetic bias Unlike web-sourced images for public presentation (e.g., recipes, advertisements, or social media), our dataset consists of casual, unfiltered photos taken for personal use. These images often feature poor lighting, unstyled plating, or partially eaten dishes—scenarios rarely encountered in web-collected data, and thus exhibit a fundamentally different visual character.

Time-series continuity for personalization Since many users log meals over extended periods, the dataset has a partial time-series structure. This temporal continuity facilitates longitudinal modeling and enables evaluation of incremental learning and personalization.

Multi-dish meal composition Each image in our dataset may contain multiple dishes that co-occur on the same plate or tray, reflecting realistic meal compositions and enabling context-aware classification based on dish co-occurrence within a single meal.

Figure 1 illustrates several of these distinguishing properties, including visual diversity, meal composition, and real-world data

characteristics. Taken together, these aspects highlight the limitations of conventional food image datasets in supporting practical food-logging applications and demonstrate the need for more realistic, user-centered resources like FoodLogAthl-218.

2 Related Works

2.1 Image-Based Food Logging

With the widespread adoption of smartphones, many meal management applications have been released. In Japan, Asken [6], MyFitnessPal [15], and Calomeal [32] are prominent. These apps utilize image recognition technology to automatically recognize the content of a meal and estimate its nutritional value.

In this research, we used the food recording app, “FoodLog Athl” [41] developed by our laboratory for academic purposes. One key feature of FoodLog Athl is its ability to facilitate communication between users and registered dietitians. Once users link their account on the app, they can share their food records with an assigned dietitian, who can then review the records and provide personalized nutritional guidance. To ensure accurate nutritional analysis, FoodLog Athl does not allow users to enter free-text dish names. Instead, users select dishes from a predefined database that contains approximately 1,400 common Japanese meals and an additional 140K items (including everyday foods, restaurant dishes, and packaged products). This database is compiled from SARAH [1] and the Standard Tables of Food Composition in Japan [47].

2.2 Food Image Datasets

For models to accurately predict real-world data, they must be trained on rich data that reflects real-world environments. Thus, datasets serve as the foundation for training and evaluating models, with their quality, scale, and diversity directly linked to model performance. In the field of dietary studies, research on food image datasets has progressed, with datasets such as Food-101 [10] containing 101,000 images across 101 classes, UEC-Food 256 [28] containing 25,088 images across 256 classes, and Food2K [40] containing 1,036,564 images across 2,000 classes, reflecting the growing scale of these datasets over the years.

As seen in Table 1, most existing food image datasets constructed for classification tasks rely on the Web, including social networking sites (SNS), as their primary data source.

Table 2: Data Filtering Process and the Number of Images, Bounding Boxes (bboxes) and Classes.

Step	Operation	#images	(diff)	#bboxes	(diff)	#classes	(diff)
0	Raw data	11,460		61,414		5,889	
1	Remove samples w/o image	11,460 (0)		26,646 (-34,768)		3,167 (-2,722)	
2	Remove samples w/o bounding box	11,285 (-175)		26,065 (-581)		3,071 (-96)	
3	Remove classes w/ <10 samples	9,121 (-2,164)		21,944 (-4,121)		1,180 (-1,891)	
4	Remove outliers based on image features	7,537 (-1,584)		17,513 (-4,431)		1,180 (0)	
5	Manual review and remove invalid images	6,925 (-612)		14,349 (-3,164)		1,180 (0)	
6	Merge similar classes and clean labels	6,925 (0)		14,349 (0)		218 (-982)	

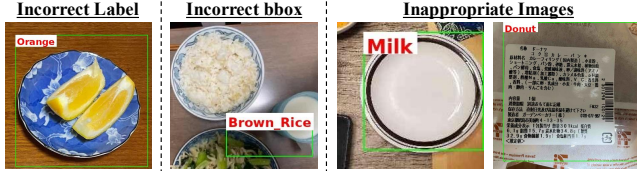


Figure 2: Examples of erroneous data.

2.3 Vision-Language Models in the Food Domain

2.3.1 CLIP. Contrastive Language–Image Pretraining (CLIP) [43] serves as a baseline for food image classification thanks to its strong zero-shot accuracy. For example, CLIP’s zero-shot classifier achieves over 90% Top-1 accuracy on Food-101 [43]—outperforming a ResNet-50-based classifier [18] by more than 15 points. Moreover, in ingredient estimation tasks, CLIP-based models yield higher per-ingredient recall and F1 scores than ResNet-based counterparts [48].

2.3.2 Large Multi-modal Models (LMMs). Beyond CLIP, recent progress in multimodal learning has centered on general-purpose LMMs, which combine image encoders and large language models into end-to-end frameworks. Models such as LLaVA [33], MiniGPT-4 [54], OpenFlamingo [7], Phi-3.5-Vision [2], and Qwen-VL [8] have all demonstrated strong zero-shot and few-shot performance across a range of food-related tasks. For example, FoodMLM-JP leverages these architectures for Japanese recipe generation with excellent fluency and culinary accuracy [23]. Domain-adapted variants—such as FoodLMM [51], ChefFusion [31], and RODE [24]—further boost fine-grained classification, ingredient localization, and nutrition estimation. These successes confirm that CLIP and LMMs serve as robust baselines for our food image benchmarks.

3 FoodLogAthl-218 Dataset

As mentioned in the Introduction, food records submitted by users in daily food-logging applications tend to be highly noisy, as shown in Figure 2. To address this, we developed a custom multi-stage filtering pipeline to extract a clean subset comparable in quality to existing food image datasets.

3.1 Data Collection

The dataset used in this study consists of food records collected via the FoodLog Athl app from May 2023 to October 2024, covering 632 users. Since many users upload only once, or submit non-food images, we applied the following filtering steps to obtain a reliable

subset of approximately 60,000 records: (i) selected dietitians linked to at least three user accounts, (ii) identified all user accounts associated with those dietitians, and (iii) retrieved every meal record from those users. Each record contains an anonymized user ID, meal date and time, dish name, portion size, an image with bounding box annotations, and nutritional values (all initially inferred by the app’s built-in detection and recognition models and then corrected by users as needed). As images often contain multiple dishes, each dish is treated as an individual sample, allowing a single image to correspond to multiple dataset samples.

3.2 Data Filtering

An overview of our data cleaning steps and their impact on sample and class counts is shown in Table 2. Steps 1 and 2 remove records with missing or incorrectly assigned images and bounding boxes. Step 3 drops underrepresented classes that are unsuitable for training.

Step 4 applies CLIP-based outlier detection to catch subtler errors such as mislabeled crops or non-food images. Each dish crop is encoded with a pre-trained CLIP model (ViT-B/16), and its feature distance from the class centroid is calculated. To choose an appropriate cutoff, we manually inspected samples across different distance ranges and found that flagging those more than 1.5 standard deviations above the class mean removed clear errors with high precision while preserving valid but uncommon cases. Accordingly, any sample whose distance exceeds this threshold is flagged as an outlier.

Step 5 manually reviews all remaining samples, correcting bounding boxes and labels or removing any invalid entries to ensure final dataset quality.

To preserve the natural distribution of food records in real-world logging, we treat each image as an atomic unit.

Since one image may contain multiple dishes, removing individual samples could distort meal-level patterns.

Instead, if any sample from an image is flagged, all associated samples are discarded.

This all-or-none policy maintains the original frequency of multi-dish meals and supports full-meal tasks, such as the description-guided classification in Section 4.3. A total of 6,925 meal images with 14,349 bounding boxes from 513 users remained after filtering up to Step 5.

Table 3: Comparison of distribution metrics between FoodLogAthl-218 and UEC-Food 256 using feature extractors. Higher *Trace* and *Davies–Bouldin* indicate greater spread, while lower *Silhouette* and *Calinski–Harabasz* indicate less compact clusters.

Dataset	Trace (↑)			Silhouette (↓)			Davies–Bouldin (↑)			Calinski–Harabasz (↓)		
	CLIP	EVA-CLIP	Swin	CLIP	EVA-CLIP	Swin	CLIP	EVA-CLIP	Swin	CLIP	EVA-CLIP	Swin
UEC-Food 256	71.21	45.09	264.00	0.0335	0.0577	-0.0064	3.64	3.02	4.11	74.05	115.80	49.17
FoodLogAthl-218 (Ours)	81.70	49.92	282.57	-0.0210	0.0036	-0.0288	4.52	3.68	4.51	27.51	51.51	21.29

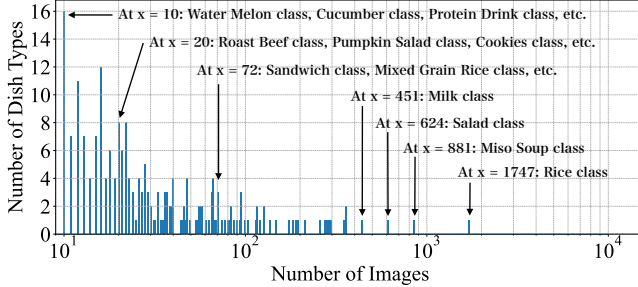


Figure 3: Log–linear plot of the number of entries per class in FoodLogAthl-218 (logarithmic horizontal axis, linear vertical axis), with illustrative examples.



Figure 4: Examples of data included in FoodLogAthl-218.

3.3 Clustering

As explained in Sec. 2.1, food names (i.e., class labels) are drawn from over 140K choices and still exhibit various notation inconsistencies after filtering. To compare our dataset with existing food image datasets, we adopted a two-stage clustering procedure in Step 6 to merge labels referring to the same dish. First, we prompted GPT-4o [3] with “Please group the following dish names into appropriate categories,” leveraging its pretrained language and domain knowledge to automatically cluster synonyms, spelling variants, and minor phrasing differences. This model-assisted step greatly reduces the manual effort needed to unify a large, noisy label set. Second, we manually reviewed and refined these clusters to correct any misgroupings and ensure that each class retained clear, distinct definitions. By combining scalable, automated grouping with targeted human curation, we achieve both efficiency and high labeling accuracy in our final class definitions.

3.4 Dataset Overview and Class Distribution

Figure 3 plots the distribution of entries per class in FoodLogAthl-218 on a log–linear scale (logarithmic horizontal axis, linear vertical axis). The number of samples per class is highly imbalanced, faithfully reflecting the true frequency distribution of daily meals logged by Japanese FoodLog Athl users.

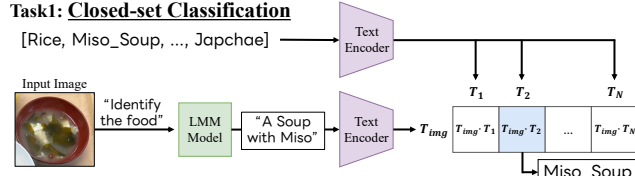
Figure 4 shows example meal images from FoodLogAthl-218. The dataset includes images that are rarely found on the web but commonly appear in personal food logs, such as boxed meals (red box) and packaged products purchased at convenience stores (blue box), as well as partially eaten rice in a rice cooker (purple box). Another notable feature is the wide variation in composition and lighting. For example, in the image outlined in yellow, the photographer’s smartphone casts a shadow over the food—a common characteristic of casual, unedited meal snapshots.

To evaluate within-class variability and between-class separability, we extracted image features from every sample in FoodLogAthl-218 and UEC-Food 256—another Japanese food image classification dataset—using three different encoders: CLIP (ViT-L/14) [43], EVA-CLIP (eva_giant_patch14_clip_224) [46], and Swin Transformer (swin_large_patch4_window12_384_ms_in22k) [34]. For each encoder and its corresponding feature set, we computed four dispersion metrics to evaluate class separability and variability:

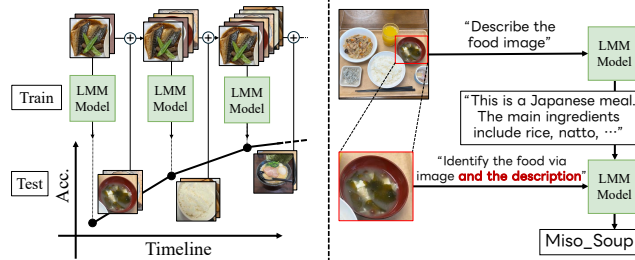
- **Trace (↑)** [25]: Sum of variances across all feature dimensions. Higher values indicate more within-class spread.
- **Silhouette Score (↓)** [44]: Measures class cohesion and separation; lower scores suggest greater overlap.
- **Davies–Bouldin Index (↑)** [13]: Ratio of within-class scatter to between-class separation. Larger values reflect less compact, more overlapping classes.
- **Calinski–Harabasz Score (↓)** [11]: Ratio of between-class to within-class variance. Lower values indicate weaker separation.

Table 3 summarizes these four metrics for each encoder. The arrows in the column headers denote the direction (↑ larger, ↓ smaller) that corresponds to higher intra-class variance and inter-class overlap, i.e., greater difficulty of classification. Across all metrics and encoders, FoodLogAthl-218 shows consistently higher intra-class variance and inter-class overlap than UEC-Food 256, demonstrating that our user-submitted, bottom-up collection yields more visual diversity (and noise) than datasets gathered via traditional web-based methods.

Task1: Closed-set Classification



Task2: Continual User-Aware Adaptation



Task3: Menu-Aware Classification

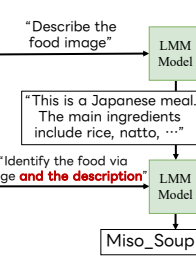


Figure 5: Overview of the three evaluation tasks.

4 Benchmark Tasks and Experimental Setup

In this section, we define three tasks to evaluate the complexity of the FoodLogAthl-218 dataset and provide baseline methods for each using large multimodal models (LMMs), as illustrated in Figure 5.

4.1 Task 1. Standard Closed-Set Classification

4.1.1 Task Definition and baseline method. As in conventional food-image benchmarks, each dish crop is assigned exactly one of the 218 class labels. We benchmarked this task across various LMMs using `lmms-eval`, a unified and standardized multimodal evaluation framework that includes more than 10 models[30, 52]. In the baseline method, we first generated a free-form description for each dish image crop, then embedded both the description and all 218 class labels using the `intfloat/e5-large-v2` text encoder [49]. The predicted label was selected as the one with the highest cosine similarity to the description embedding. This overall pipeline is illustrated at the top of Figure 5. For EVA-CLIP and CLIP, classification was performed by directly computing cosine similarity between the image features and label text embeddings. We report Top-1/3/5 accuracy to account for uncertainty and label ambiguity.

4.1.2 Experimental Results. Table 4 shows that GPT-4o achieves the highest recall@1 ($\approx 42\%$), and among all open-source models Qwen2.5-VL-7B-Instruct is strongest, but even the best LMMs stall around 40% recall@1, highlighting the challenge of FoodLogAthl-218. Interestingly, a smaller-scale classification model compared to LMMs, CLIP (ViT-L/14) attains the top recall@5 (60%). This stems from its direct image–text similarity scoring, which naturally produces a full ranked list, whereas embedding-based LMM descriptions tend to concentrate probability on their first guess and are less effective at generating diverse Top-N candidates.

4.2 Task 2. Continual User-Aware Adaptation

4.2.1 Task Definition and Baseline Method 1. Users often exhibit repetitive eating patterns, frequently consuming similar meals over time. This suggests that continuously updating a model with newly

Table 4: Classification performance on FoodLogAthl-218.

Model	F1	R@1	R@3	R@5
GPT-4o	0.3732	0.4243	0.4991	0.5221
Qwen2.5-VL-7B-Instruct	0.2349	0.3684	0.4609	0.4859
Qwen2-VL-7B-Instruct	0.1594	0.3656	0.4590	0.4781
Qwen2-VL-3B-Instruct	0.1386	0.2663	0.3250	0.3517
llava-onevision-qwen2-7b-ov	0.1546	0.3629	0.4497	0.4639
EVA-CLIP (ViT-g)	0.2465	0.2654	0.4897	0.5944
CLIP (ViT-L/14)	0.2393	0.2567	0.4885	0.6000
llava-v1.6-34b	0.1354	0.2432	0.3779	0.4063
llava-v1.5-7b	0.0991	0.2140	0.2721	0.2973
llava-v1.6-mistral-7b	0.0944	0.1932	0.2595	0.2831

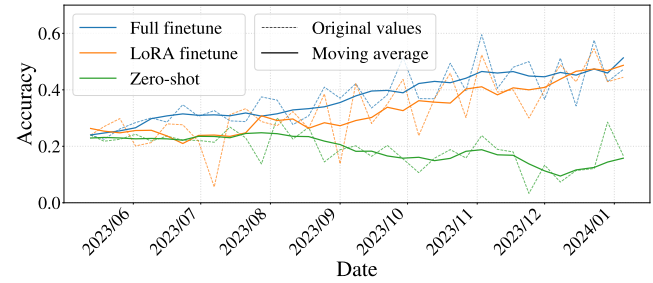


Figure 6: Incremental accuracy: zero-shot, full fine-tuning, and LoRA fine-tuning on all users.

logged meals could improve classification performance, as previously seen meals become easier to recognize. Using the “meal date” metadata, we incrementally fine-tuned a model on all records up to week $n - 1$ and tested on meals logged in week n , as illustrated at the bottom left of Figure 5.

Using Qwen2.5-VL-3B-Instruct, we evaluated three model variants on held-out splits: (1) full fine-tuning, (updates all model parameters), (2) LoRA fine-tuning (adapts only low-rank adapter weights) [22], and (3) a zero-shot baseline with no fine-tuning.

4.2.2 Experimental Results 1. Figure 6 shows incremental accuracy for the three variants. Solid lines represent a weighted one-month moving average (\pm two weeks) with weights proportional to the number of weekly records; dotted lines plot the raw weekly accuracy.

Figure 6 shows that with continual fine-tuning on real meal logs, accuracy climbs from roughly 20% to over 50%—a gain of more than 30 percentage points over the zero-shot baseline—ultimately surpassing even large commercial LMMs. LoRA fine-tuning, though slightly behind full fine-tuning in the earliest weeks when only a few dozen records are available, quickly catches up as more data accumulates, achieving near-full-finetune performance with only a small fraction of trainable parameters. In contrast, the zero-shot curve slowly drifts downward, highlighting the importance of users’ dietary history updates in counteracting the distributional shift in real-world meal-logging data.

4.2.3 Task Definition and Baseline Method 2. To analyze the impact of long-term logging on personalization, we focused on the single most active user (User A), who consistently logged meals from May

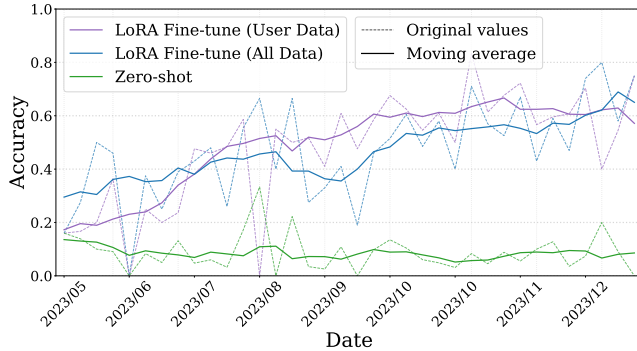


Figure 7: User A accuracy over time: zero-shot, LoRA fine-tuned on all users, and LoRA fine-tuned on User A only.

Table 5: F1 score, Precision@1 (P@1), and Recall@K (R@1, R@3, R@5) for Qwen2.5-VL-7B-Instruct on the description-guided classification task.

	F1	P@1	R@1	R@3	R@5
w/o description	0.1594	0.1019	0.3656	0.4590	0.4781
w/ description	0.2304	0.1788	0.3240	0.4032	0.4336

12, 2023 to January 12, 2024, submitting 274 images covering 1,003 dish entries. On this user’s records, we compared three variants: (1) LoRA fine-tuned solely on User A’s data, (2) LoRA fine-tuned on all users, and (3) zero-shot baseline with no fine-tuning.

4.2.4 Experimental Results 2. Figure 7 shows their classification accuracy on User A’s records over time. Solid curves represent a one-month moving average (\pm two weeks), while dotted curves plot the raw weekly accuracy.

From Figure 7, both LoRA-fine-tuned models ultimately deliver a 50 percentage points increase over the zero-shot baseline. The all-data model initially outperforms the user-specific model, but as more entries from User A accumulate, the personalized model closes the gap—eventually matching or surpassing the all-data model—demonstrating effective user-level adaptation.

4.3 Task 3. Menu-Aware Classification

4.3.1 Task Definition and Baseline Methods. A single photo often contains several dishes. To leverage this context, we first show the whole image to the LMM and ask for a short “menu” description summarizing every visible item. Each crop is then re-evaluated with both its own image and the menu description. This two-stage inference uses meal-level cues to distinguish visually similar dishes—e.g., mains vs. sides or regional variants—and aims to boost per-dish accuracy. This overall pipeline is illustrated at the bottom right of Figure 5.

4.3.2 Experimental Results. We used Qwen2.5-VL-7B-Instruct to generate menu descriptions. Table 5 shows the model’s F1, Precision@1 (P@1), and Recall@K (R@1, R@3, R@5) when classifying each dish crop with and without a high-level meal description.

Adding the menu description raises F1 from 0.159 to 0.230 and boosts Precision@1 by over 7.5% (from 0.102 to 0.179), at the cost of a modest drop in Recall. As one illustrative example, the model—rather

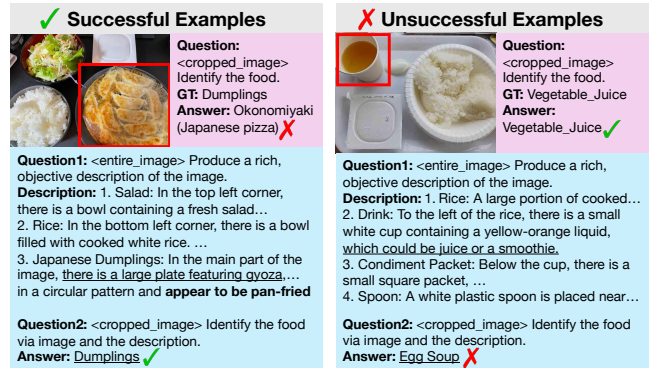


Figure 8: Illustrative examples for the description-guided classification task. Pink-shaded regions show the baseline “without description” setting, while blue-shaded regions show the “with description” setting.

than defaulting to “Rice” (11.9% of samples)—now correctly predicts rarer variants like Barley_Rice, Brown_Rice, and Fried_Rice. Crucially, this is not limited to the Rice class: comparable reductions in bias toward other dominant labels and shifts toward their less common subcategories are observed across the dataset, demonstrating a general improvement in label diversity.

Despite this improvement, the addition of menu descriptions also introduces trade-offs: it correctly reclassifies 687 previously misclassified instances but simultaneously misclassifies 1,222 instances that were originally labeled correctly. Figure 8 presents representative examples of both successful corrections and new errors. These results suggest that the LMM effectively utilizes contextual information from the full meal. For example, a cropped image of gyoza is incorrectly classified as okonomiyaki when evaluated in isolation. However, with the addition of the full-meal description, which mentions rice and side dishes, items typically served with gyoza but not with okonomiyaki in Japan, the model correctly predicts the label Dumplings. Conversely, some samples that were correctly classified without context become misclassified once the meal description is included, indicating that while context can enhance prediction accuracy, it can also introduce ambiguity or mislead the model in some instances.

5 Conclusion

We presented *FoodLogAth1-218*, a 6,925-image, 14,349 bounding box, and 218-class food dataset derived from real meal logs with rich metadata and natural class imbalance. Through three tasks—closed-set classification, continual user-aware adaptation, and description-guided classification—we demonstrated that state-of-the-art LMMs struggle with raw food-log data but improve significantly through incremental and context-aware fine-tuning.

Availability. *FoodLogAth1-218* is released for non-commercial academic research. Access requires an institutional e-mail. Request it at <https://huggingface.co/datasets/FoodLog/FoodLogAth1-218> via “Apply”; credentials are issued after a short manual review.

Ethics Statement This study was approved by the Ethics Review Committee of the Graduate School of Information Science and Technology, The University of Tokyo (protocol **UT-IST-RE-250415-2**).

6 Acknowledgements

This work was supported by JSPS KAKENHI Grant Number 23K25247 and JST NEXUS, Japan Grant Number JPMJNX25C9.

References

- [1] 2025. SARAH. <https://corporate.sarah30.com/>. (Accessed on 29/05/2025).
- [2] Marah Abdin, Jyoti Aneja, Hany Awadalla, Ahmed Awadallah, Ammar Ahmad Awan, Nguyen Bach, Amit Bahree, Arash Bakhtiari, Jianmin Bao, Harkirat Behl, et al. 2024. Phi-3 technical report: A highly capable language model locally on your phone. *arXiv preprint arXiv:2404.14219* (2024).
- [3] Josh Achiam, Steven Adler, Sandhini Agarwal, Lama Ahmad, Ilge Akkaya, Florencia Leoni Aleman, Diogo Almeida, Janko Altenschmidt, Sam Altman, Shyamal Anadkat, et al. 2023. Gpt-4 technical report. *arXiv preprint arXiv:2303.08774* (2023).
- [4] Kiyoharu Aizawa, Yuto Maruyama, He Li, and Chamin Morikawa. 2013. Food Balance Estimation by Using Personal Dietary Tendencies in a Multimedia Food Log. *IEEE Trans. Multimedia* 15, 8 (2013), 2176–2185.
- [5] Marios M Anthimopoulos, Lauro Gianola, Luca Scarnato, Peter Diem, and Stavroula G Mougialakou. 2014. A food recognition system for diabetic patients based on an optimized bag-of-features model. *JBHI* 18, 4 (2014), 1261–1271.
- [6] asken, Inc. 2007. Asken (originally in Japanese). <https://www.asken.jp/>. (Accessed on 16/03/2024).
- [7] Anas Awadalla, Irena Gao, Josh Gardner, Jack Hessel, Yusuf Hanafy, Wanrong Zhu, Kalyani Marathe, Yonatan Bitton, Samir Gadre, Shiori Sagawa, et al. 2023. Openflamingo: An open-source framework for training large autoregressive vision-language models. *arXiv preprint arXiv:2308.01390* (2023).
- [8] Jinze Bai, Shuai Bai, Yunfei Chu, Zeyu Cui, Kai Dang, Xiaodong Deng, Yang Fan, Wenbin Ge, Yu Han, Fei Huang, et al. 2023. Qwen technical report. *arXiv preprint arXiv:2309.16609* (2023).
- [9] Thoranna Bender, Simon Sørensen, Alireza Kashani, Kristjan Eldjarn Hjorleifsson, Grethe Hyldig, Søren Hauberg, Serge Belongie, and Frederik Warburg. 2024. Learning to taste: A multimodal wine dataset. *NeurIPS* 36 (2024).
- [10] Lukas Bossard, Matthieu Guillaumin, and Luc Van Gool. 2014. Food-101-mining discriminative components with random forests. In *ECCV*.
- [11] T. Caliński and J. Harabasz. 1974. A Dendrite Method for Cluster Analysis. *Communications in Statistics – Theory and Methods* 3, 1 (1974), 1–27.
- [12] Mei Chen, Kapil Dhingra, Wen Wu, Lei Yang, Rahul Sukthankar, and Jie Yang. 2009. PFID: Pittsburgh fast-food image dataset. In *ICIP*.
- [13] D. L. Davies and D. W. Bouldin. 1979. A Cluster Separation Measure. *IEEE Transactions on Pattern Analysis and Machine Intelligence PAMI-1*, 2 (1979), 224–227.
- [14] Jia Deng, Wei Dong, Richard Socher, Li-Jia Li, Kai Li, and Li Fei-Fei. 2009. Imagenet: A large-scale hierarchical image database. In *CVPR*.
- [15] Daniel Evans. 2017. MyFitnessPal. *BJSM* 51, 14 (2017), 1101–1102.
- [16] Giovanni Maria Farinella, Dario Allegra, Marco Moltisanti, Filippo Stanco, and Sebastiano Battiatto. 2016. Retrieval and classification of food images. *Computers in biology and medicine* 77 (2016), 23–39.
- [17] Google LLC. 2024. Google Search. <https://www.google.com/>. (Accessed on 16/03/2024).
- [18] Kaiming He, Xiangyu Zhang, Shaoqing Ren, and Jian Sun. 2016. Deep residual learning for image recognition. In *CVPR*.
- [19] Hajime Hoashi, Taichi Joutou, and Keiji Yanai. 2010. Image recognition of 85 food categories by feature fusion. In *ISM*.
- [20] Shinji Horiguchi, Sosuke Amano, Masahiko Ogawa, and Kiyoharu Aizawa. 2018. Personalized Classifier for Food Image Recognition. *IEEE Trans. Multimedia* 20, 10 (2018), 2836–2848.
- [21] Saini Hou, Yushan Feng, and Zilei Wang. 2017. Vegfru: A domain-specific dataset for fine-grained visual categorization. In *ICCV*.
- [22] Edward J Hu, Yelong Shen, Phillip Wallis, Zeyuan Allen-Zhu, Yuanzhi Li, Shean Wang, Lu Wang, Weizhi Chen, et al. 2022. Lora: Low-rank adaptation of large language models.. In *ICLR*, Vol. 1. 3.
- [23] Yuki Imajuku, Yoko Yamakata, and Kiyoharu Aizawa. 2025. FoodMLM-JP: Leveraging Multimodal Large Language Models for Japanese Recipe Generation. In *MMM 2025*, 401–414. doi:10.1007/978-981-96-2054-8_30
- [24] Pengkun Jiao, Xinlan Wu, Bin Zhu, Jingjing Chen, Chong-Wah Ngo, and Yugang Jiang. 2024. RoDE: Linear Rectified Mixture of Diverse Experts for Food Large Multi-Modal Models. *arXiv preprint arXiv:2407.12730* (2024).
- [25] I. T. Jolliffe. 2002. *Principal Component Analysis*. Springer.
- [26] Taichi Joutou and Keiji Yanai. 2009. A food image recognition system with multiple kernel learning. In *ICIP*.
- [27] Parneet Kaur, Karan Sikka, Weijun Wang, Serge Belongie, and Ajay Divakaran. 2019. Foodx-251: a dataset for fine-grained food classification. In *Fine-Grained Visual Categorization Workshop, CVPR*.
- [28] Y. Kawano and K. Yanai. 2014. Automatic Expansion of a Food Image Dataset Leveraging Existing Categories with Domain Adaptation. In *ECCV Workshops (TASK-CV)*.
- [29] Seum Kim, Yoko Yamakata, and Kiyoharu Aizawa. 2021. Boosting Personalized Food Image Classifier by Sharing Food Records. In *ACM ICMR Workshops*, 29–32.
- [30] Bo Li, Peiyuan Zhang, Kaichen Zhang, Fanyi Pu, Xinrun Du, Yuhao Dong, Haotian Liu, Yuanhan Zhang, Ge Zhang, Chunyuan Li, and Ziwei Liu. 2024. LMMs-Eval: Accelerating the Development of Large Multimodal Models. <https://github.com/EvolvingLMMs-Lab/lmms-eval>
- [31] Peiyu Li, Xiaobao Huang, Yijun Tian, and Nitesh V Chawla. 2024. Cheffusion: Multimodal Foundation Model Integrating Recipe and Food Image Generation. In *CIKM*, 3872–3876.
- [32] Life Log Technology, Inc. 2016. calomeal (originally in Japanese)". <https://www.calomeal.com/about-calomeal/>. (Accessed on 16/03/2024).
- [33] Haotian Liu, Chunyuan Li, Qingyang Wu, and Yong Jae Lee. 2024. Visual instruction tuning. *NeurIPS* 36 (2024).
- [34] Ze Liu, Yutong Lin, Yue Cao, Han Hu, Yixuan Wei, Zheng Zhang, Stephen Lin, and Baining Guo. 2021. Swin transformer: Hierarchical vision transformer using shifted windows. In *ICCV*, 10012–10022.
- [35] Zheng Ma, Mianzhi Pan, Wenhan Wu, Kanzhi Cheng, Jianbing Zhang, Shujian Huang, and Jiajun Chen. 2023. Food-500 Cap: A Fine-Grained Food Caption Benchmark for Evaluating Vision-Language Models. In *ACMMM*.
- [36] Yuji Matsuda and Keiji Yanai. 2012. Multiple-food recognition considering co-occurrence employing manifold ranking. In *ICPR*.
- [37] Meituan. 2024. Meituan. <https://www.meituan.com/>. (Accessed on 16/03/2024).
- [38] Weiqing Min, Linhu Liu, Zhengdong Luo, and Shuqiang Jiang. 2019. Ingredient-guided cascaded multi-attention network for food recognition. In *ACMMM*.
- [39] Weiqing Min, Linhu Liu, Zhiling Wang, Zhengdong Luo, Xiaoming Wei, Xiaolin Wei, and Shuqiang Jiang. 2020. Isia food-500: A dataset for large-scale food recognition via stacked global-local attention network. In *ACMMM*.
- [40] Weiqing Min, Zhiling Wang, Yuxin Liu, Mengjiang Luo, Liping Kang, Xiaoming Wei, Xiaolin Wei, and Shuqiang Jiang. 2023. Large scale visual food recognition. *TPAMI* (2023).
- [41] Kei Nakamoto, Kohei Kumazawa, Hiroaki Karasawa, Sosuke Amano, Yoko Yamakata, and Kiyoharu Aizawa. 2022. FoodLog Athl: Multimedia Food Recording Platform for Dietary Guidance and Food Monitoring. In *ACMMM Asia*.
- [42] Jianing Qiu, Frank P-W Lo, Yingnan Sun, Siyao Wang, and Benny Lo. 2019. Mining discriminative food regions for accurate food recognition. *BMVC* (2019).
- [43] Alec Radford, Jong Wook Kim, Chris Hallacy, Aditya Ramesh, Gabriel Goh, Sandhini Agarwal, Girish Sastry, Amanda Askell, Pamela Mishkin, Jack Clark, et al. 2021. Learning transferable visual models from natural language supervision. In *ICML*.
- [44] P. J. Rousseeuw. 1987. Silhouettes: A graphical aid to the interpretation and validation of cluster analysis. *J. Comput. Appl. Math.* 20 (1987), 53–65.
- [45] Doyen Sahoo, Wang Hao, Shu Ke, Wu Xiongwei, Hung Le, Palakorn Achananuparp, Ee-Peng Lim, and Steven CH Hoi. 2019. FoodAI: Food image recognition via deep learning for smart food logging. In *KDD*.
- [46] Quan Sun, Yuxin Fang, Ledell Wu, Xionlong Wang, and Yue Cao. 2023. EVA-CLIP: Improved Training Techniques for CLIP at Scale. *arXiv preprint arXiv:2303.15389* (2023). <https://arxiv.org/abs/2303.15389>
- [47] The Japanese Ministry of Education, Culture, Sports, Science and Technology. 2015. *STANDARD TABLES OF FOOD COMPOSITION IN JAPAN - 2015 - (Seventh Revised Version)*. <https://www.mext.go.jp/en/policy/science-technology/policy/title01/detail01/1374030.htm> (Accessed on 21/07/2024).
- [48] Liangyu Wang, Yoko Yamakata, Ryoma Maeda, and Kiyoharu Aizawa. 2024. Measure and Improve Your Food: Ingredient Estimation Based Nutrition Calculator. In *ACM MM '24*, 11273–11275. doi:10.1145/3664647.3684997
- [49] Liang Wang, Nan Yang, Xiaolong Huang, Binxing Jiao, Linjun Yang, Daxin Jiang, Rangan Majumder, and Furu Wei. 2022. Text Embeddings by Weakly-Supervised Contrastive Pre-training. *arXiv preprint arXiv:2212.03533* (2022). <https://arxiv.org/abs/2212.03533>
- [50] Xin Wang, Devinder Kumar, Nicolas Thome, Matthieu Cord, and Frederic Precioso. 2015. Recipe recognition with large multimodal food dataset. In *ICMEW*.
- [51] Yuehai Yin, Huiyan Qi, Bin Zhu, Jingjing Chen, Yu-Gang Jiang, and Chong-Wah Ngo. 2023. FoodLmm: A versatile food assistant using large multi-modal model. *arXiv preprint arXiv:2312.14991* (2023).
- [52] Kaichen Zhang, Bo Li, Peiyuan Zhang, Fanyi Pu, Joshua Adrian Cahyono, Kairui Hu, Shuai Liu, Yuanhan Zhang, Jingkang Yang, Chunyuan Li, and Ziwei Liu. 2024. LMMs-Eval: Reality Check on the Evaluation of Large Multimodal Models. *arXiv:2407.12772 [cs.CL]* <https://arxiv.org/abs/2407.12772>
- [53] Feng Zhou and Yuanqing Lin. 2016. Fine-grained image classification by exploring bipartite-graph labels. In *CVPR*.
- [54] Deyao Zhu, Jun Chen, Xiaoqian Shen, Xiang Li, and Mohamed Elhoseiny. 2023. Minigpt-4: Enhancing vision-language understanding with advanced large language models. *arXiv preprint arXiv:2304.10592* (2023).